Mesenchymal stem cells polarize macrophages to an anti-inflammatory phenotype to ameliorate diabetic nephropathy

Linxi Zhang (zhanglinxi99@163.com)
Peking University Third Hospital https://orcid.org/0000-0002-5185-9742

Songyan Yu
Beijing Tiantan Hospital

Yu Cheng
Chinese PLA General Hospital

Zhengyuan Gong
Army Medical University Xinqiao Hospital

Jing Xue
PLA Strategic Support Force Characteristic Medical Center

Bing Li
Chinese PLA General Hospital

Yaqi Yin
Chinese PLA General Hospital

Junyan Zou
Chinese PLA General Hospital

Rui Wei
Peking University Third Hospital

Tianpei Hong
Peking University Third Hospital

Yiming Mu
Chinese PLA General Hospital https://orcid.org/0000-0002-3344-3540

Research Article

Keywords: Diabetic nephropathy, mesenchymal stem cell, macrophages, inflammation, fibrosis

Posted Date: August 23rd, 2022

DOI: https://doi.org/10.21203/rs.3.rs-1965742/v1

Abstract

Background

Diabetic nephropathy is closely related to immune-regulation, in which macrophages play a crucial role. In diabetic nephropathy, the classically activated macrophages (M1) increased while the alternatively activated macrophages (M2) decreased in kidney. Mesenchymal stem cells (MSCs) administration can alleviate diabetic nephropathy, however, the mechanisms still remain unclear. MSCs have been shown to stimulate macrophages from a M1 phenotype to a M2 phenotype. Thus, we aimed to investigate whether the polarization of M1/M2 induced by MSCs was involved in diabetic nephropathy (DN).

Methods

In our study, we injected human umbilical cord mesenchymal stem cells (UC-MSCs) into type 2 diabetic nephropathy rats induced by high fat diet combined with a low dose of streptozotocin. To clarify the effect of MSCs on macrophages polarization, peritoneal macrophages were extracted and directed into M1 macrophages by lipopolysaccharides (LPS) in vitro. Then we co-cultured UC-MSCs with M1 macrophages, and evaluated the effect on differentiation. We also co-cultured rat glomerular mesangial cells (HBZY-1) in high-glucose DMEM with LPS-stimulated macrophages (M1 macrophages) or UC-MSCs-induced M2 macrophages in a trans-well system to clarify the complex mechanisms by which UC-MSCs-induced M2 macrophages improve the progression of DN.

Results

The UC-MSCs infusion reduced the infiltration of M1 macrophages, and increased the infiltration of M2 macrophages in the glomerulus, thereby attenuating histopathological renal damage and improving renal inflammation and fibrosis in diabetic nephropathy rats. After coculturing UC-MSCs with M1 macrophages, we found that the M1 macrophage maker inducible nitric oxide synthase (NOS2) and the mRNA and protein levels of the related pro-inflammatory cytokines TNF-α, TGF-β and IL-1β decreased. However, the expression of the M2 macrophage markers CD163 and CD206, as well as the anti-inflammatory cytokine IL-10 increased observably. Furthermore, UC-MSCs increased the expression of IL-4Rα on macrophages by secreting IL-6; blocking IL-6 secretion inhibited the UC-MSCs effect on M2 macrophage polarization. Then we explored the mechanism by which M2 macrophages ameliorate diabetic nephropathy in vitro and found that UC-MSCs-induced M2 macrophages attenuated the secretion of the chemokine monocyte chemoattractant protein-1(MCP-1) in hyperglycemia-induced mesangial cells, which led to reduce macrophage recruitment and infiltration. Moreover, UC-MSCs-induced M2 macrophages inhibited TGF-β in glomerular mesangial cells, thereby reducing the synthesis of collagen I and collagen IV.

Conclusions

Our study proposes and discusses a mechanism by which MSCs promote the polarization of macrophages from M1 into M2 in the kidney, thereby ameliorating diabetic nephropathy.

Introduction

Diabetic nephropathy (DN) is one of the most serious complications of diabetes mellitus, it occurs in 20–40% of diabetic patients and is the most common cause of end-stage chronic kidney disease.[1–3] DN is morphologically characterized by thickening of the glomerular basement membrane (GBM), mesangial expansion and glomerulosclerosis, leading to proteinuria, hypertension and a decreased glomerular filtration rate. Despite current treatment may prevent or delay the development of DN, the identification of new methods for the treatment of DN based on the pathophysiological mechanism is necessary.

Evidence has suggested that macrophages, as key inflammatory cells, play a crucial role in the pathogenesis of DN.[4–6] In human progressive DN, macrophages accumulate within glomeruli and the interstitium, and the intensity of the macrophages infiltration is associated with the rate of subsequent decline in renal function. [4] Another study demonstrated that MCP-1-mediated macrophage accumulation and activation plays a critical role in the development of streptozotocin (STZ)-induced mouse DN. [5] Macrophages are characterized as having M1 and M2 phenotypes. Classically activated M1 macrophages are broadly characterized as being pro-inflammatory, while alternatively activated M2 macrophages are involved in tissue repair and remodeling. [7–10] M1 macrophages positively correlate with the progression of DN, in contrast, M2 macrophages protect renal function in DN. [11–14] Therefore, promoting the polarization of macrophages in the kidney may be a new strategy for DN.

Mesenchymal stem cells (MSCs) have previously been reported to halt the progression of DN by improving the inflammatory microenvironment, but the underlying mechanism remains elusive. [15] Notably, MSCs have diverse potential therapeutic applications for different organs and tissues via interactions with components of both the innate and adaptive immune systems. MSCs have been shown to stimulate macrophages from a primarily pro-inflammatory M1 phenotype to a more anti-inflammatory M2 phenotype both in vitro and in vivo.[16–18] Our previous study demonstrated that MSCs promoted M2 polarization to alleviate insulin resistance and repair β-cell function. [19–21] However, the role of MSCs in modulating macrophage polarization and related DN has not been reported. Therefore, in the current study, we explored the mechanism by which human umbilical cord mesenchymal stem cells (UC-MSCs) promote the polarization of macrophages from the M1 to the M2 phenotype in the kidney, thereby ameliorating DN. Our findings provide a theoretical basis for the wide use of MSCs in future clinical treatment of DN in patients with diabetes mellitus.

Methods

Animal experiments

Eight-week-old male SD rats were fed a high-fat diet (HFD) or normal-chow diet (NCD) for 8–9 weeks. The body weight of HFD rats was maintained at 600 g, and a low dose of STZ (22mg/kg) was injected to induce type 2 diabetes mellitus (T2DM). Intraperitoneal glucose tolerance tests (IPGTTs) and insulin tolerance tests (IPITTs) were performed to confirm T2DM (Figure S1). HFD rats were then fed a HFD for another 8 weeks to mimic the early stages of human DN. A total of 3×10^6 MSCs suspended in 0.5 ml of phosphate-buffered saline (PBS) were infused via the tail vein every 2 weeks (referred to as the MSC group), whereas T2DM (DM group) and NCD (N group) rats were infused with PBS as a control. The treatments were performed four times in total. All in vivo procedures were approved by the Medical Ethics Committee of the Chinese PLA General Hospital.

Cell Culture

Human umbilical cords were obtained from healthy women who gave birth at the Chinese PLA General Hospital. All subjects provided informed consent. The Ethics Committee of the Chinese PLA General Hospital approved the study. The isolation and identification of human UC-MSCs has been previously described by our team. [19–21]

Peritoneal macrophages were obtained from SD rats by peritoneal lavage with H-DMEM (Gibco, USA) for 7–10 min. The macrophage purity assessed by anti-F4/80 immunofluorescence was greater than 90%. After 1×10^5 peritoneal macrophages were seeded onto six-well plates for 12 h, 1 μg/ml lipopolysaccharides (LPS; Sigma-Aldrich) was added for 24 h. The macrophages were then cultured with 3×10^4 UC-MSCs in a trans-well system for 48 h. For IL-6 neutralization experiments, 0.1μg/ml IL-6 neutralizing antibody (NA; R&D Systems, USA) was added to the culture medium when UC-MSCs were co-cultured with macrophages. The UC-MSCs and culture medium IL-6 levels were detected by quantitative real-time reverse transcriptase polymerase chain reaction (qRT-PCR) and enzyme-linked immunosorbent assay (ELISA) to confirm the successful blockade of IL-6.

Rat glomerular mesangial cells (HBZY-1) were purchased from the Basic Medical Cell Center (Institute of Basic Medicine, Chinese Academy of Medical Sciences). HBZY-1 cells were cultured in L-DMEM (Gibco, USA) supplemented with 10% FBS for 12 h, and then the medium was replaced with H-DMEM (Gibco, USA) containing 10% FBS. After 12 or 24 h of stimulation, increasing IL-1β, TGF-β and collagen I/IV levels were measured to mimic the glucotoxicity of glomerular mesangial cells.

Biochemical tests for albuminuria

Urine excreted from each animal was collected using a metabolic cage system. Albuminuria levels were measured using immune-turbidimetric methods, and creatinine levels were measured using enzymatic methods. The urinary albumin levels were normalized to the urinary creatinine levels (albumin creatine ratio, ACR).

Immunohistochemistry staining and Immunofluorescence Staining

The animals were euthanized with chloral hydrate (10%, 3ml/kg). The right kidney was removed for immunoblotting and qRT-PCR tests, and the animal was perfused with 4% paraformaldehyde through the aortic trunk cannulated by the left ventricle. The fixed kidney was embedded in paraffin, and the sections of 10 μm thickness were cut and stained with hematoxylin and eosin (H&E), Masson, periodic acid Schiff (PAS) and Sirius red according to standard protocols. Glomerular damage was expressed as the percentage of glomeruli presenting mesangial expansion and glomerulosclerosis. For staining of collagen I/IV, fibronectin, IL-1β,TNF-α, TGF-β, CD68, CD206, CD11c and CD163, kidney samples were immersed in 4% paraformaldehyde and paraffin-embedded sections were incubated with primary antibodies and biotinylated secondary antibody. (Supplementary Table S1) The positively stained area of the images were calculated by Image Pro plus 6.0 software (Microsoft Media Cybernetics, USA). The area of positively stained region represented the mean density of each image in different groups of renal tissue.

Kidney ultrastructure evaluation

Electron microscopy was used to evaluate the ultrastructure of GBM and the podocytic processes. Fresh kidney tissue was fixed in 1% glutaraldehyde, followed by 1% osmium tetroxide and uranyl acetate and finally embedded in epoxy resin. The specimens were examined and photographed using a transmission electron microscope (JEM-1400EX, Japan) at 3000, 5000 and 30000× magnification at an accelerating voltage of 80 kV. Electron micrographs were randomly taken from three glomeruli per kidney, and the kidneys were also randomly taken from three rats of each group.

Immunoblotting

The proteins extracted from tissues and cells were assessed by Western blotting; 10% SDS-polyacrylamide electrophoresis and nitrocellulose membranes were used. The membranes were blocked with 5% none-fat milk and incubated with primary antibodies (Supplementary Table S2) at 4°C overnight, followed by incubation with a secondary antibody. β-Actin was used as a loading control for comparison between samples. Image J software (NIH, USA) was used to analyze the blots.

Quantitative real-time reverse transcriptase polymerase chain reaction

Total RNA from tissues and cultured cells was extracted using TRIzol reagent (Life Technolopies, 15596018, USA) and a reverse transcription kit (Thermo Fisher, K1622, USA) in accordance with the manufacturer's protocols. An ABI Prism thermal cycler (model StepOne- Plus; Applied Biosystems, CA, USA) and SYBR Green PCR Master Mix (Applied Biosystems) were used to quantify target genes (Supplementary Table S3). β-Actin was used as the internal control. All the reactions were performed in duplicate.

Enzyme-linked Immunosorbent Assay

The levels of TNF-α stimulated gene 6 (TSG-6), indoleamine 2,3-dioxygenase (IDO), IL-6 and TGF-β secreted by UC-MSCs were measured using commercial ELISA kits (NeoBioscience, China) according to the manufacturer's instructions.

Statistical analysis

The data were expressed as the mean ± SD from at least three independent samples. The values were analyzed using one-way ANOVA followed by two-tailed Student's t tests. The differences between the mean values were considered significant when the two-tailed p value was < 0.05. SPSS 19.0 (SPSS Inc., IBM, USA) was used for statistical analysis.

Results

UC-MSCs therapy improved glucose homeostasis and inhibited the increase of albuminuria in diabetic rats.

UC-MSCs were identified by osteogenic and adipogenic differentiation. (Fig. 1A) The flow cytometry analysis showed that UC-MSCs expressed high levels of surface CD73, CD90 and CD105, but lacked surface CD45, CD34 and HLA-DR. (Fig. 1B) The T2DM rat model was induced with a combination of an 8-9week HFD and a single intraperitoneal injection of a low dose of STZ (Supplementary Figure S1). The high-fat diet was fed to HFD rats for a further 8 weeks to mimic the early stages of human DN. A total of 3 X 10^6 MSCs suspended in 0.5 ml of PBS were infused via the tail vein every 2 weeks (referred as the MSC group), whereas T2DM (DM group) and NCD (N group) rats were infused with PBS as a control. The treatments were performed four times in total (Fig. 1C). After 4 weeks of treatment, the random blood glucose level in the MSC group was 387.45 ± 20.70 mg/dl, which was lower than the 446.40 ± 30.93 mg/dl of the DM group of (Fig. 1D). The body weight of the MSC group increased more than that of the DM group (Fig. 1E). The IPGTT results showed that MSC treatment alleviated glucose tolerance and insulin tolerance (Fig. 1F,G) and significantly increased insulin sensitivity (Fig. 1H,I), suggesting a marked improvement in glucose homeostasis.

Urine excreted by each animal was collected using a metabolic cage system after STZ injection and MSC treatment at a fixed time. The ACR after STZ injection and before MSC treatment showed no significant difference in each group. The ACR in the DM group was elevated slightly at 4 weeks after MSC administration (P = 0.032), and elevated significantly at 7 weeks after MSC administration (P = 0.001) compared with that in the MSC treatment group, revealing MSC infusions inhibited the increase in albuminuria in diabetic rats.

UC-MSCs therapy attenuated histopathological damage in diabetic rats.

H&E staining demonstrated that DM group rats had notable glomerular hypertrophy, glomerulosclerosis and mesangial matrix expansion compared with the normal group and MSC group rats. Masson staining showed renal fibrosis, and PAS staining showed fibrous protein, mesangial matrix and amyloid protein in diabetic rats, nevertheless, these changes were markedly reduced in the MSC treatment group. Sirius-red staining also showed no renal fibrosis in MSC group (Collagen-positive area by Sirius = 27.92 ± 3.29%) compared with the DM group (36.87 ± 4.59%, P = 0.006; Fig. 2A). Transmission electron microscopy (TEM) was used for the ultrastructural assessment of glomerular injury (Fig. 2B). Consistent with our histologic findings, TEM indicated mesangial matrix deposition, local podocyte effacement, GBM thickening and endothelial cell proliferation in diabetic rats, whereas MSC treatment improved these changes dramatically.

UC-MSCs therapy ameliorated renal fibrosis in diabetic rats.

Renal fibrosis is the final outcome of progressive DN. To investigate the impact of UC-MSCs on renal fibrosis, we detected the expression of the main extracellular matrix (ECM) components, including collagen I, collagen IV and fibronectin in kidney by immunohistochemical staining. The ECM component-positive area in the UC-MSCs therapy rats was significantly reduced compared with that in diabetic rats (Fig. 3A). The protein expression of collagen I decreased, moreover, the mRNA expression of collagen I, collagen IV and α-SMA declined remarkably after UC-MSCs therapy in the MSC group compared with the DM group (Fig. 3B, C). In summary, these results demonstrate that UC-MSCs infusion reduced renal fibrosis.

UC-MSCs therapy ameliorated renal inflammation in diabetic rats.

Considerable evidence indicates that inflammation plays a critical role in renal fibrosis, accelerating the progression of DN. We measured pro-inflammation cytokines, which are well-known markers of DN. The IL-1β, TNF-α and TGF-β positive areas detected by immunohistochemical staining in the MSC group were smaller than those in the DM group (Fig. 4A). Additionally, Western-blotting showed reduced protein expression of TNF-α and TGF-β after UC-MSCs administration (Fig. 4B). The mRNA expression of pro-inflammation cytokines, including TNF-α, TGF-β, IL-1β, EP-4 and STAT3, was downregulated by UC-MSCs therapy compared with the no-therapy condition. In addition, UC-MSCs promoted anti-inflammatory cytokine IL-10 mRNA upregulation in the kidney (Fig. 4C), suggesting that UC- MSCs have strong immunosuppressive effects on DN.

UC-MSCs therapy induced M2 macrophage polarization in the kidney of diabetic rats.

Macrophages, as key inflammatory cells accumulating within glomeruli, are associated with renal damage in DN. Therefore, we investigated the effects of UC-MSCs on macrophages in diabetic rats. Immunohistochemical staining revealed that there were more CD68 positive macrophages (regardless of sub-phenotype) and fewer CD11c (an M1marker)-positive macrophages in the DM group than in the MSC group. However, there were more CD206 (an M2 marker)-positive macrophages and more CD163 (an M2 marker)-positive macrophages in the MSC group than in the DM and N groups (Fig. 5A). The mRNA

expression of monocyte chemoattractant protein (MCP-1), which is involved in macrophage infiltration, was elevated in diabetic rats. In addition, CD68, NOS2 (an M1marker) and CD206 mRNA expression detected by RT-PCR was consistent with the results of immunohistochemical staining, demonstrating that UC-MSCs reduced the infiltration of total macrophages and induced M2 macrophage phenotype polarization in the kidneys of diabetic rats (Fig. 5B).

UC-MSCs suppressed M1 macrophage polarization and induced M2 macrophage polarization in vitro.

To confirm the effects of UC-MSCs on M2 macrophage polarization, we extracted peritoneal macrophages from SD rats and verified that more than 95% of cells were F4/80-positive (a marker for macrophages regardless of sub-phenotypes) (Fig. 6A). Light microscopy revealed that LPS administration induced the extension of many pseudopodia by macrophages. After co-culture with UC-MSCs, fewer macrophage pseudopodia were observed in vitro (Fig. 6B). LPS administration induced peritoneal macrophages to express more iNOS (a marker for M1) and less Arg 1 (a marker for M2) than coculture with UC-MSCs, suggesting that LPS polarized peritoneal macrophages to M1 phenotypes, whereas UC-MSCs suppressed M1 polarization and induced M2 macrophages polarization. The Western-blotting results also showed a higher expression level of Arg 1 in the UC-MSCs co-culture group than in the LPS group (Fig. 6C, D). Consistently, the mRNA expression of the M1 macrophage maker NOS2 and the related pro-inflammatory cytokines TNF-α, TGF-β and IL-1β decrased after UC-MSCs co-culture. mRNA expression of the M2 macrophage markers CD163 and CD206 and anti-inflammatory cytokine IL-10, increased observably in the MSC group (Fig. 6E).

UC-MSCs induced M2 macrophage polarization via IL-6/IL-4R in vitro.

Previous studies have shown that MSC-mediated polarization of M2 macrophages depends on the secretion of prostaglandin E2 (PGE2), TSG-6, IL-6, IDO and TGF-β1.[16–18, 22] We analyzed the mRNA expression of these genes in UC-MSCs to investigate the possible factors responsible for M2 macrophage polarization and found that only IL-6 was significantly elevated (Fig. 7A). When UC-MSCs were co-cultured with LPS-stimulated macrophages from 12h to 48h, the level of IL-6 secreted from UC-MSCs increased gradually (Fig. 7B). Then, we used an IL-6 NA to reduce IL-6 to an extremely low level to determine whether IL-6 induces M2 macrophage polarization (Fig. 7C, D). According to the immunofluorescence results, Arg1 expression was markedly decreased after IL-6 neutralization (Fig. 7E). IL-4 and IL-13 have been demonstrated to be the major cytokines mediating M2 macrophage polarization via IL-4Rα overexpression. Nevertheless, IL-4/IL-13 were extremely low, and IL-4Rα protein expression in macrophages was upregulated after MSC co-culture but downregulated significantly after IL-6 neutralization (Fig. 7F). Together, these studies reveal that the UC-MSCs effect on M2 polarization is mediated by IL-6/IL-4Rα.

UC-MSCs-induced M2 macrophages protect HBZY-1 from high-glucose toxicity.

To clarify the complex mechanisms by which UC-MSCs-induced M2 macrophages improve the progression of DN, we used HBZY-1 to further elucidate the mechanisms in vitro (Fig. 8A). According to

the immunofluorescence analysis, compared with the other groups, the group cultured with high-glucose DMEM for 24 h showed the highest collagen I expression (Fig. 8B). Similarly, the mRNA expression of IL-1β, TGF-β, collagen I and collagen IV were increased by culturing with high glucose concentrations for 24 h (Fig. 8C). We next co-cultured HBZY-1 in high-glucose DMEM with LPS-stimulated macrophages (M1 macrophages) or UC-MSCs-induced M2 macrophages in a trans-well system. As expected, the M2 macrophages markedly reduced collagen I expression compared with M1 macrophages (Fig. 8D). NADPH oxidase 4(NOX-4)/TGF-β1 signaling activation mediates the accumulation of ECM. [23] UC-MSCs induced M2 macrophages downregulated NOX-4, TGF-β and collagen I protein expression (Fig. 8E) and reduced collagen I, collagen IV, IL-1β and CCL2 (involved in macrophages infiltration) mRNA expression (Fig. 8F). Taken together, the results provide strong evidence that UC-MSCs induced M2 macrophages may be in the development of DN (Fig. 9).

Discussion

Our current study provides strong evidence that UC-MSCs were involved directly in DN by inducing M2 macrophage polarization. MSCs have been lauded as a novel therapeutic strategy for diabetes mellitus and its complications, because MSCs have several advantages, for instance, their ability to migrate to injured tissues, immune-suppressive effects and safely properties. [24–26] Because relatively few MSCs migrate to the kidneys, previous studies concentrated on the immune-regulatory function of MSCs, such as reducing oxidative stress, increasing the secretion of anti-apoptotic cytokines, suppression inflammation, producing anti-inflammatory mediators and producing growth factors, leading to the amelioration of ECM accumulation and renal damages. [15, 27–28] Despite the paracrine effects of MSCs on the prevention of DN having been previously documented, the molecular crosstalk mechanism between MSCs and macrophages remains unclear. Consistent with previous studies, MSCs infusion ameliorated renal injury by suppressing inflammation, as demonstrated by the downregulation of IL-1β, TNF-α and TGF-β in our study. Notably, macrophages were the major inflammatory cell type in the development of DN. Similarly, the classically activated macrophage (M1) proportion increased while the alternatively activated macrophage (M2) proportion decreased in the kidney in DN. M1 macrophages are characterized by the overexpression of pro-inflammatory cytokines; in contrast, M2 macrophages are considered to be involved in immune-regulatory functions. Interestingly, we demonstrated that UC-MSCs decreased the number of M1 macrophages but increased the number of M2 macrophages in STZ-induced diabetic rats. Furthermore, UC-MSCs-induced M2 macrophages protect glomerular mesangial cells from high-glucose toxicity in vitro. Therefore, the therapeutic effects of UC-MSCs on DN were partially attributed to macrophage polarization phenotype.

Macrophages play a crucial role in inflammation, while distinct functional phenotypes of macrophages are acquired depending on the microenvironment. M1 macrophages are induced by Toll-like receptor (TLR) ligands and Interferon γ (IFN-γ) and are characterized by the production of pro-inflammatory factors, including TNF-α, IL-1β, IL-6, IL-12, and proteolytic enzymes. M2 macrophages are induced by IL-4 and IL-13, and secrete anti-inflammatory cytokines, such as TGF-β, IL-1 receptor antagonist and IL-10. [7–

[10] Recent studies have demonstrated that M1 macrophages switch to M2 macrophages under certain circumstances.[8, 29] Interestingly, MSCs have been reported to induce M2 macrophages polarization according to the secretion of soluble factors, including PGE2, TSG-6, IL-6, IDO, and TGF-β1. [16–18, 22] Furthermore, IL-4/IL-13/IL-4Rαoverexpression has been documented in M2 polarized macrophages. [30] The different cytokines secreted by MSCs may be related to diverse inflammatory environments. In our study, UC-MSCs promoted the polarization of macrophages from M1 to M2 by secreting IL-6, and blocking IL-6 secretion inhibited the UC-MSCs effect on M2 macrophages polarization. However, we found that IL-4 and IL-10 levels were extremely low in MSCs-mediated M2 macrophages, but the expression of IL-4Rα on macrophages increased significantly. Previous studies have indicated that IL-4Rαplays a crucial role in M2 macrophage polarization. [31] Our results reveal that MSCs suppress M1 macrophages and induce M2 macrophage polarization via IL-6/IL-4Rα.

Recent studies have revealed that different versions of M2 macrophages, including M2a, M2b and M2c, have diverse functional states. In particular, M2a, induced by IL-4 and IL-13 (high Arg, CD163 and CD206 expression, low IL-1, IL-6, TNF-αand TGF-βexpression), and M2b, induced by immune complexes and TLR or IL-1R agonists (high IL-1, IL-6 and TNF-αexpression, low CD163, CD206 and TGF-βexpression), both exert immune-regulatory functions and drive type II responses. M2c macrophages, induced by IL-10 (high CD163, CD206 and TGF-βexpression, low IL-1, IL-6 and TNF-αexpression), are predominantly related to suppression of immune responses and tissue remodeling.[32–33] MSCs-mediated M2 macrophages were generally characterized by increased expression of CD206 and CD163 and reduced expression of IL-1β,TNF-αand TGF-β, suggesting that MSCs may induced M2a phenotype macrophage polarization. Mesangial expansion is a characteristic feature of DN and closely correlates with ECM deposition and inflammation, leading to renal decline. Mesangial cells exposure to high glucose concentrations increases the expression of collagen and fibronectin, and the secretion of cytokines, such as transforming growth factor-beta 1 (TGF-β), connective tissue growth factor (CTGF), vascular endothelial growth factor (VEGF), and monocyte chemoattractant protein-1 (MCP-1). [34] In our study, MSCs-mediated M2 macrophages inhibited collagen I/IV, TGF-βand IL-1βin mesangial cells in high glucose conditions. Interestingly, MCP-1 was also decreased by M2 macrophages in vivo and vitro to reduce the infiltration of monocytes and macrophages. In addition, Nox-4 is a Nox family NADPH and is a major source of reactive oxygen species in the diabetic kidney. [35] Nox-4 participates in high glucose-mediated mitochondrial ROS generation in mesangial cells and induces ECM accumulation via TGF-βsignaling, which is a key regulator of ECM deposition that acts by enhancing the synthesis of collagen and fibronectin, as well as by inhibiting ECM degradation. [22,36] We found that MSCs-mediated M2 macrophages inhibited Nox-4/TGF-β/collagen I signaling in mesangial cells; however, further exploration is needed.

Conclusion

The UC-MSCs infusion reduced the infiltration of M1 macrophages, and increased the infiltration of M2 macrophages in the glomerulus, thereby attenuating histopathological renal damage and improving renal

inflammation and fibrosis in diabetic nephropathy. These results provide a theoretical basis for the use of MSCs in clinical treatment of DN in patients with diabetes mellitus in the future.

Abbreviations

M1:Classically activated macrophages; M2:Alternatively activated macrophages; MSCs: Mesenchymal stem cells; DN: Diabetic nephropathy; UC-MSCs: Human umbilical cord mesenchymal stem cells; LPS: Lipopolysaccharides; HBZY-1: Rat glomerular mesangial cells; NOS2: Inducible nitric oxide synthase; TNF-α:Tumor necrosis factor α; TGF-β: Transforming growth factor β; MCP-1: Monocyte chemoattractant protein-1; GBM: Glomerular basement membrane; STZ: Streptozotocin; HFD: High-fat diet; NCD: Normal-chow diet; T2DM: Type 2 diabetes mellitus; IPGTTs: Intraperitoneal glucose tolerance tests; IPITTs: Insulin tolerance tests; PBS: Phosphate-buffered saline; qRT-PCR: Quantitative real-time reverse transcriptase polymerase chain reaction; ELISA: Enzyme-linked immunosorbent assay; ACR: Albumin creatine ratio; H&E: Hematoxylin and eosin; PAS: Periodic acid Schiff; TSG-6: TNF-α stimulated gene 6; IDO: Indoleamine 2,3-dioxygenase; TEM: Transmission electron microscopy; ECM: Extracellular matrix; iNOS: Inducible nitric oxide synthase; PGE2: Prostaglandin E2; NOX-4: NADPH oxidase 4; TLR: Toll-like receptor; IFN-γ: Interferon γ; CTGF: Connective tissue growth factor; VEGF: Vascular endothelial growth factor.

Declarations

Ethics approval and consent to participate

All animal experiment protocols were approved by the medical ethics committee of the Chinese PLA General Hospital.

Consent for publication

Not applicable

Availability of data and material

The datasets used and/or analysed during the current study are available.

Competing interests

The authors declare that they have no competing interests.

Funding

This work was supported in National Natural Science Foundation of China [81870578, 81900754, 82170875and 82100861].

Acknowledgements

We thank the technical assistance from Jiejie Liu, Qi Zhang, and other members of the Mu laboratories for insightful discussions over this work.

Authors' contributions

LZ, SY and YC contributed to the conception and design, provision of study material, collection of data, data analysis and interpretation, and manuscript writing. ZG, JX and BL contributed to the provision of study material and collection of data. QY and YZ contributed to the collection of data and data analysis and interpretation. RW contributed to the provision of study material and data analysis and interpretation. YM and PH contributed to the conception and design, financial support, manuscript writing, and final approval of manuscript. LZ, SY and YC contributed equally to this article. All authors read and approved the final manuscript.

References

1. Parving HH, Lewis JB, Ravid M, Remuzzi G, Hunsicker LG; DEMAND investigators. Prevalence and risk factors for microalbuminuria in a referred cohort of type II diabetic patients: a global perspective. Kidney Int, 2006, 69(11):2057-63.
2. Maisonneuve P, Agodoa L, Gellert R, Stewart JH, Buccianti G, Lowenfels AB, et al. Distribution of primary renal diseases leading to end-stage renal failure in the United States, Europe, and Australia/New Zealand: Results from an international comparative study. Am J Kidney Dis, 2000, 35:157-65.
3. Jia W, Gao X, Pang C, Hou X, Bao Y, Liu W, et al. Prevalence and risk factors of albuminuria and chronic kidney disease in Chinese population with type 2 diabetes and impaired glucose regulation: Shanghai diabetic complications study (SHDCS). Nephrol Dial Transplant, 2009, 24:3724-31.
4. Awad AS, You H, Gao T, Cooper TK, Nedospasov SA, Vacher J, et al. Macrophage-derived tumor necrosis factor-α mediates diabetic renal injury. Kidney Int. 2015, 88(4).
5. Chow FY, Nikolic-Paterson DJ, Ma FY, Ozols E, Rollins BJ, Tesch GH. Monocyte chemoattractant protein-1-induced tissue inflammation is critical for the development of renal injury but not type 2 diabetes in obese db/db mice. Diabetologia, 2007, 50(2):471-80.
6. Klessens CQ, Zandbergen M, Wolterbeek R, Bruijn JA, Rabelink TJ, Bajema IM, et al. Macrophages in diabetic nephropathy in patients with type 2 diabetes. Nephrol Dial Transplant, 2017, 32(8):1322-9.
7. Gordon S. Alternative activation of macrophages. Nat Rev Immunol, 2003, 3:23–35.
8. Bouhlel MA, Derudas B, Rigamonti E, Dièvart R, Brozek J, Haulon S, et al. PPARgamma activation primes human monocytes into alternative M2 macrophages with anti-inflammatory properties. Cell Metab, 2007, 6(2):137-43.
9. Benoit M, Desnues B, Mege J L. Macrophage polarization in bacterial infections. J Immunol, 2008, 181:3733-9.

10. Martinez FO, Helming L, Gordon S. Alternative activation of macrophages: an immunologic functional perspective. Annu. Rev. Immunol. 2009, 27:451-83.
11. Wang X, Yao B, Wang Y, Fan X, Wang S, Niu A, et al. Macrophage Cyclooxygenase-2 Protects Against development of Diabetic Nephropathy. Diabetes, 2017, 66(2):494-504.
12. You H, Gao T, Cooper TK, Brian Reeves W, Awad AS. Macrophages directly mediate diabetic renal injury. Am J Physiol Renal Physiol, 2013, 305(12): F1719-27.
13. Zhang XL, Guo YF, Song ZX, Zhou M. Vitamin D prevents podocyte injury via regulation of macrophage M1/M2 phenotype in diabetic nephropathy rats. Endocrinology, 2014, 155(12):4939-5490.
14. Sun H, Tian J, Xian W, Xie T, Yang X. Pentraxin-3 Attenuates Renal Damage in Diabetic Nephropathy by Promoting M2 Macrophage Differentiation. Inflammation, 2015, 38(5):1739-47.
15. Paulini J, Higuti E, Bastos RM, Gomes SA, Rangel ÉB. Mesenchymal Stem Cells as Therapeutic Candidates for Halting the Progression of Diabetic Nephropathy. Stem Cells Int. 2016;2016:9521629.
16. Nemeth K, Leelahavanichkul A, Yuen PS, Mayer B, Parmelee A, Doi K, et al. Bone marrow stromal cells attenuate sepsis via prostaglandin E(2)-dependent reprogramming of host macrophages to increase their interleukin-10 production, Nat Med, 2009, 15:42-9.
17. Francois M, Romieu-Mourez R, Li M, Galipeau J. Human MSC suppression correlates with cytokine induction of indoleamine 2,3-dioxygenase and bystander M2 macrophage differentiation. Mol Ther, 2012, 20:187-95.
18. Choi H, Lee RH, Bazhanov N, Oh JY, Prockop DJ. Anti-inflammatory protein TSG-6 secreted by activated MSCs attenuates zymosan-induced mouse peritonitis by decreasing TLR2/NF-kappaB signaling in resident macrophages. Blood, 2011, 118(2): 330-8.
19. Yu SY, Cheng Y, Zhang LX, Yin YQ, Xue J, Li B, et al. Treatment with adipose tissue-derived mesenchymal stem cells exerts anti-diabetic effects, improves long-term complications, and attenuates inflammation in type 2 diabetic rats. Stem Cell Research & Therapy, 2019,10:333.
20. Zhang YQ, Le X, Zheng S, Zhang K, He J, Liu MT, et al. MicroRNA-146a-5p-modifed human umbilical cord mesenchymal stem cells enhance protection against diabetic nephropathy in rats through facilitating M2 macrophage polarization. Stem Cell Research & Therapy, 2022, 13:171.
21. Xie ZY, Hao HJ, Tong C, Cheng Y, Liu JJ, Pang YP, et al. Human umbilical cord-derived mesenchymal stem cells elicit macrophages into an anti-inflammatory phenotype to alleviate insulin resistance in type 2 diabetic rats. Stem Cells, 2016, 34 (3):627-39.
22. Si YL, Zhao YL, Hao HJ, Liu JJ, Guo YL, Mu YM, et al. Infusion of mesenchymal stem cells ameliorates hyperglycemia in type 2 diabetic rats: identification of a novel role in improving insulin sensitivity. Diabetes, 2012, 61(6): 1616-25.
23. Yin YQ, Hao HJ, Cheng Y, Zang L, Li JJ, Gao JQ, et al. Human umbilical cord-derived mesenchymal stem cells direct macrophage polarization to alleviate pancreatic islets dysfunction in type 2 diabetic mice. Cell Death and Disease 2018, 9:760.

24. Melief SM, Geutskens SB, Fibbe WE, Roelofs H. Multipotent stromal cells skew monocytes towards an anti-inflammatory interleukin-10-producing phenotype by production of interleukin-6. Haematologica. 2013 Jun;98(6):888-95.
25. Papadimitriou A, Peixoto EB, Silva KC, Lopes de Faria JM, Lopes de Faria JB. Inactivation of AMPK mediates high phosphate-induced extracellular matrix accumulation via NOX4/TGFß-1 signaling in human mesangial cells. Cell Physiol Biochem. 2014;34(4):1260-72.
26. Le Blanc K, Mougiakakos D. Multipotent mesenchymal stromal cells and the innate immune system. Nat Rev Immunol, 2012, 12:383-96.
27. Griffin MD, Elliman SJ, Cahill E, English K, Ceredig R, Ritter T. Concise review: adult mesenchymal stromal cell therapy for inflammatory diseases: how well are we joining the dots? Stem Cells, 2013, 31:2033-41.
28. Shi YF, Wang Y, Li Q, Liu KL, Hou JQ, Shao CS, Wang Y. Immunoregulatory mechanisms of mesenchymal stem and stromal cells in inflammatory diseases. Nat Rev Nephrol. 2018, 14(8):493-507.
29. Ebrahim N, Ahmed IA, Hussien NI, Dessouky AA, Farid AS, Elshazly AM, et al. Mesenchymal Stem Cell-Derived Exosomes Ameliorated Diabetic Nephropathy by Autophagy Induction through the mTOR Signaling Pathway. Cells. 2018, 22;7(12).
30. Li DG, Wang N, Zhang L, Zhu HY, Bai XY, Bo F, et al. Mesenchymal stem cells protect podocytes from apoptosis induced by high glucose via secretion of epithelial growth factor. Stem Cell Res Ther. 2013;4(5):103.
31. Shan B, Wang XX, Wu Y, Xu C, Xia ZX, Dai JL, et al. The metabolic ER stress sensor IRE1α suppresses alternative activation of macrophages and impairs energy expenditure in obesity. Nat Immunol. 2017, 18(5):519-29.
32. Mauer J,Chaurasia B,Goldau J, Vogt MC, Ruud J, Nguyen KD, et al. Signaling by IL-6 promotes alternative activation of macrophages to limit endotoxemia and obesity-associated resistance to insulin. Nat Immunol. 2014, 15(5):423-30.
33. Zhang MZ, Wang X, Wang Y, Niu A, Wang S, Zou C, et al. IL-4/IL-13–mediated polarization of renal macrophages/dendritic cells to an M2a phenotype is essential for recovery from acute kidney injury. Kidney Int, 2017, 91(2):375-86.
34. Mantovani A, Sica A, Sozzani S, Allavena P, Vecchi A, Locati M. The chemokine system in diverse forms of macrophage activation and polarization. Trends Immunol. 2004, 25(12):677-86.
35. Spiller KL, Anfang RR, Spiller KJ, Ng J, Nakazawa KR, Daulton JW, et al.The role of macrophage phenotype in vascularization of tissue engineering scaffolds. Biomaterials. 2014, 35(15):4477-88.
36. Gruden G, Perin PC, Camussi G. Insight on the pathogenesis of diabetic nephropathy from the study of podocyte and mesangial cell biology. Curr Diabetes Rev. 2005, 1(1):27-40.
37. Gorin Y, Block K, Hernandez J, Bhandari B, Wagner B, Barnes JL, et al. Nox4 NAD(P) H oxidase mediates hypertrophy and fibronectin expression in the diabetic kidney. J Biol Chem, 2005, 280(47):39616-26.

38. Fujii M, Inoguchi T, Maeda Y, Sasaki S, Sawada F, Saito R, et al. Pitavastatin ameliorates albuminuria and renal mesangial expansion by downregulating NOX4 in db/db mice. Kidney Int, 2007, 72(4):473-80.

Figures

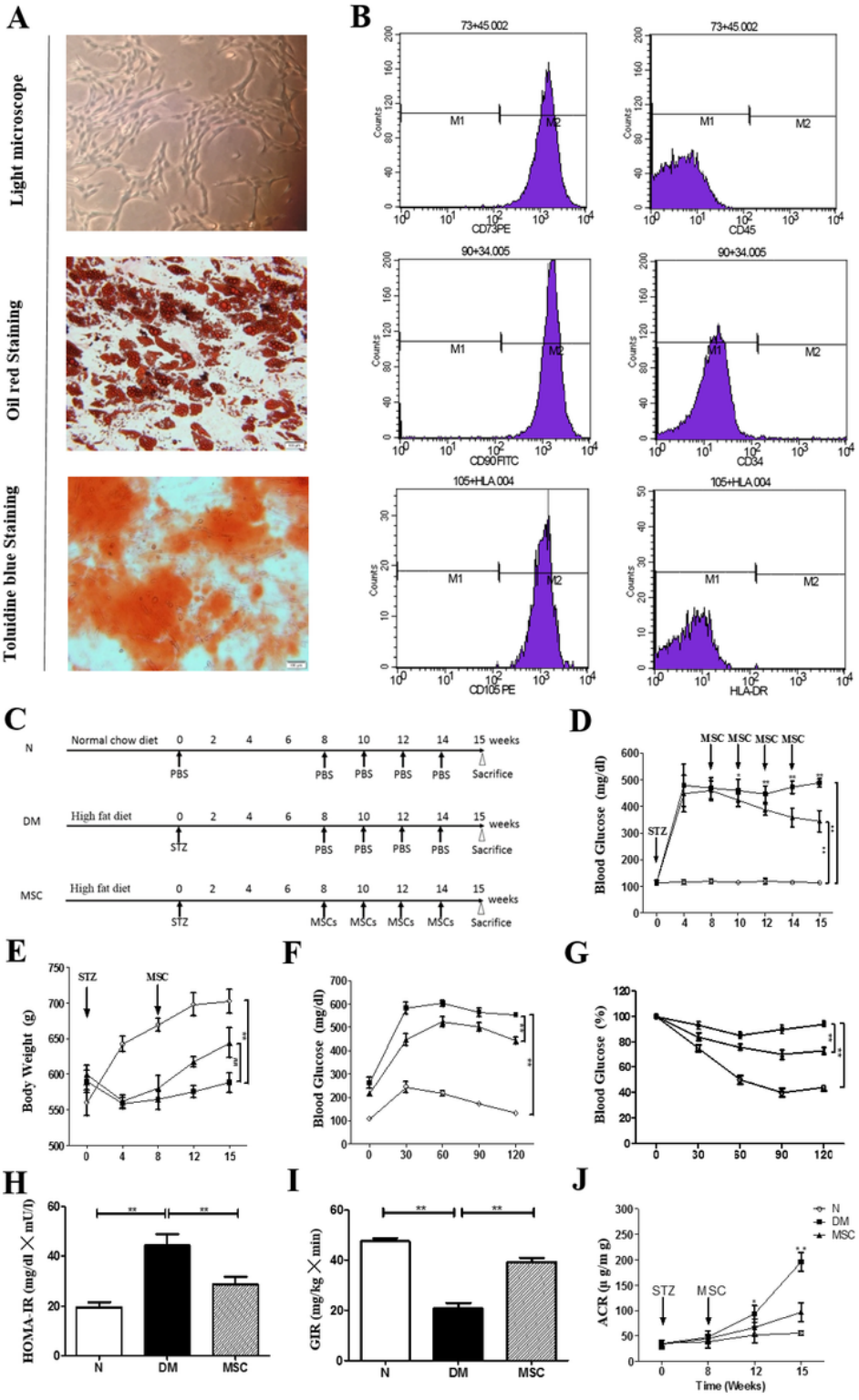

Figure 1

UC-MSCs therapy improved glucose homeostasis and inhibited the increase in albuminuria in diabetic rats.

A Capacity for differentiation to osteoblasts and adipocytes.

B The ELISA analysis of UC-MSCs surface molecules showed high levels of CD73, CD90 and CD105, and the absence of CD45, CD34 and HLA-DR.

C Experimental protocol for UC-MSCs therapy in high-fat diet diabetic rats.

D Random blood glucose levels were detected at 4, 8, 10, 12, 14 and 15 weeks after STZ infusion.

E Body weight levels were measured at 4, 8, 12 and 15 weeks after STZ infusion.

F Blood glucose concentration of three groups after IPGTT.

G Insulin tolerance was evaluated by IPITT.

H HOMA-IR index of each group.

I Glucose-infusion rate during hyperinsulinemic-euglycemic clamp analysis of three groups.

J The urinary albumin to creatinine ratio (ACR) were assessed before and after MSC treatment.

Data are expressed as mean ± SD. *p<0.05; **p<0.01; and ***p<0.001.

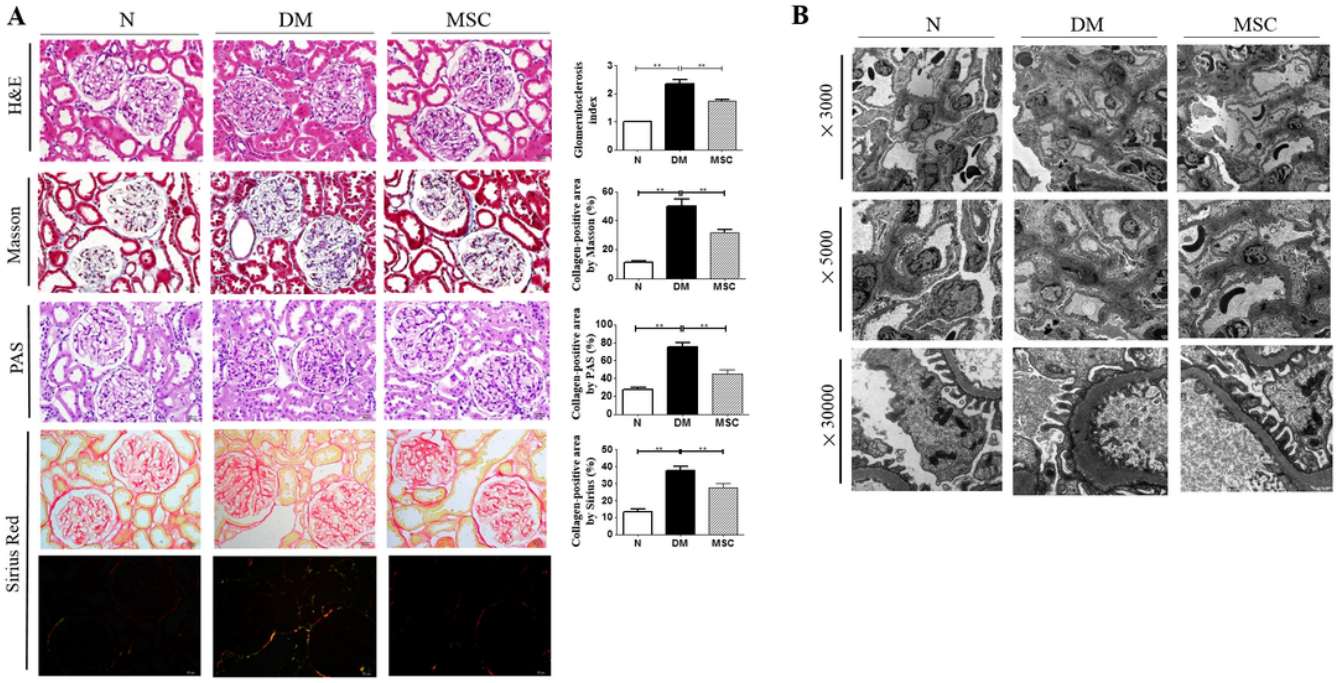

Figure 2

UC-MSCs therapy attenuated histopathological damage in diabetic rats.

(A) Histological characteristics of the kidney sections in H&E, Masson, PAS and Sirius red staining at 7 weeks after MSC administration. The scores of histological staining were calculated.

(B) Transmission electron micrographs of kidney samples are shown. (magnification: 3000, 5000, 30000.)

Data are expressed as mean ± SEM. *p<0.05; **p<0.01; and ***p<0.001.

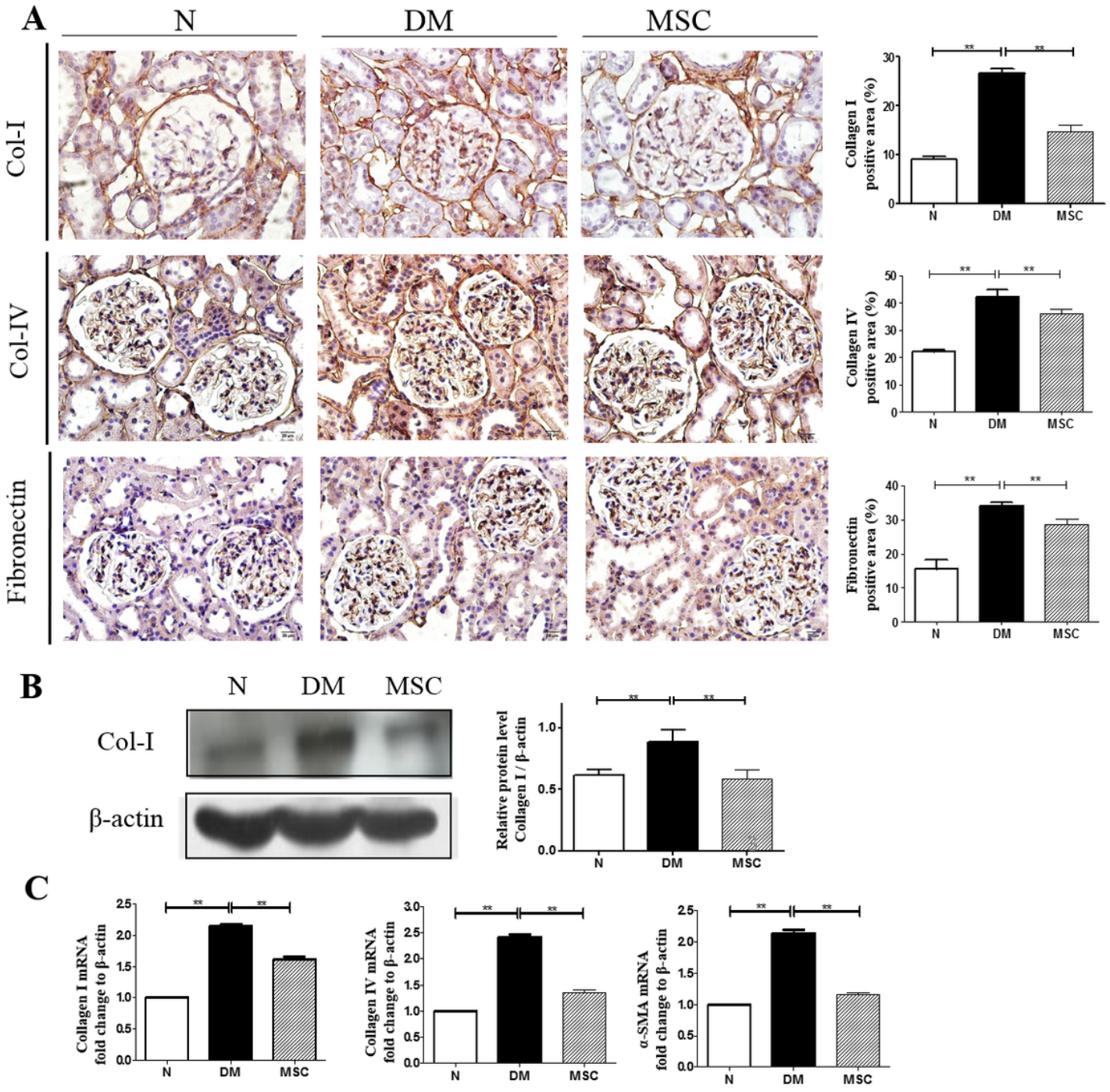

Figure 3

UC-MSCs therapy ameliorated renal fibrosis in diabetic rats.

(A) The expression of collagen I, collagen IV and fibronectin in the kidney was determined by immunohistochemistry assays.

(B) Immunoblotting analysis of collagen I was tested. The ratios of collagen I to β-actin were quantitated.

(C) Collagen I, collagen IV and fibronectin mRNA expression were evaluated by real-time PCR.

Data are expressed as mean ± SEM. *p<0.05; **p<0.01; and ***p<0.001.

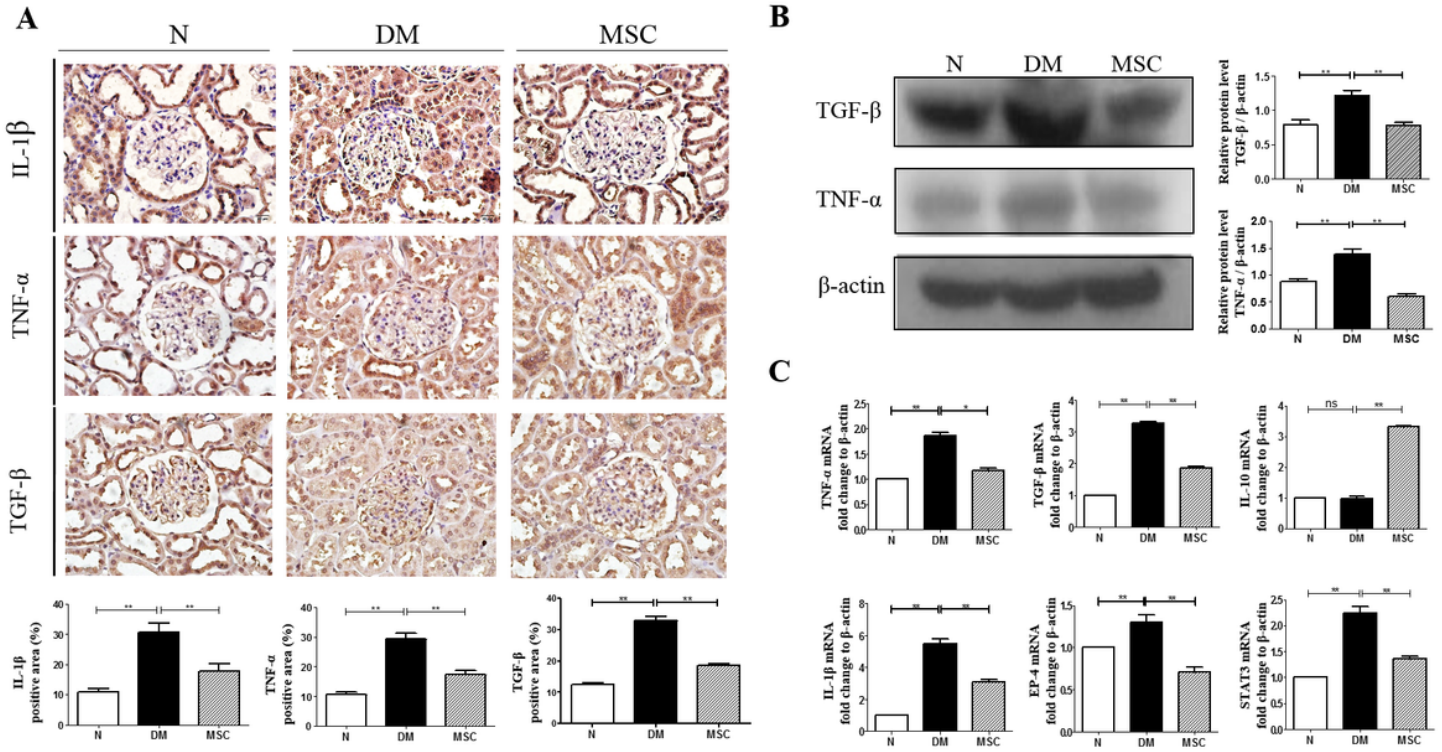

Figure 4

UC-MSCs therapy ameliorated renal inflammation in diabetic rats.

(A) Immunohistochemistry analysis of the expression of IL-1β, TNF-α and TGF-βin the kidney.

(B) Immunoblotting analysis of TGF-β and TNF-αin the kidney. Relative protein levels are quantified by the ratio of TGF-βto β-actin and TNF-α to β-actin.

(C) Quantitative reverse transcriptase polymerase chain reaction analysis of TNF-α, TGF-β, IL-10, IL-1β, EP-4 and STAT3 gene expression in kidney tissues are presented relative to those of normal rats.

Data are expressed as mean ± SD. *p<0.05; **p<0.01; and ***p<0.001.

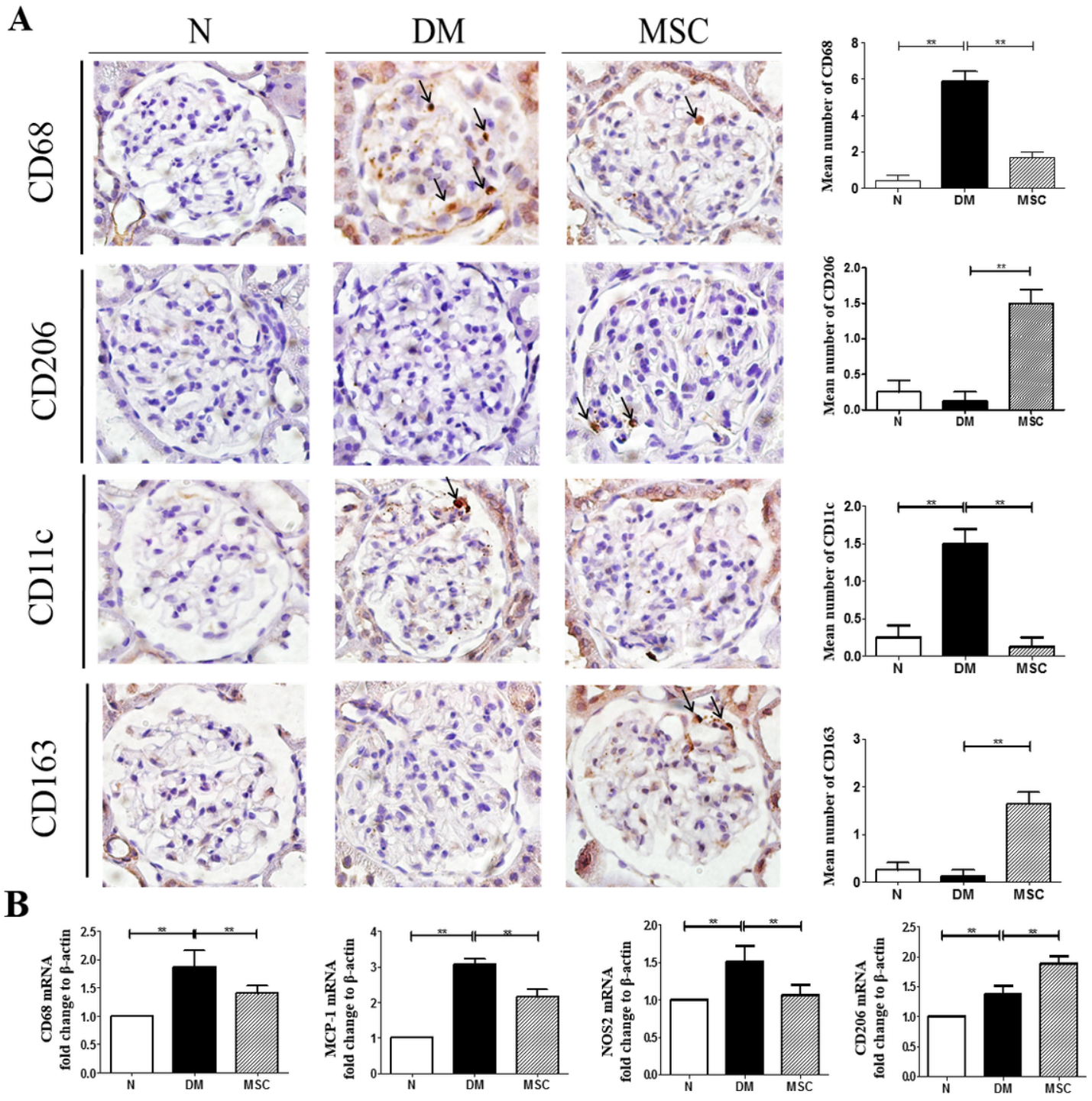

Figure 5

UC-MSCs therapy induced M2 macrophage polarization in the kidney in diabetic rats.

(A) Immunohistochemical staining of CD68 (marker for total macrophages), CD206 and CD163 (markers for M2 macrophages), and CD11c (marker for M1 macrophages) in the kidney of rats from the Nor, DM and MSC groups.

(B) Quantitative RT-PCR analysis of gene expression in the kidney from the three groups. The results are presented relative to those of the control group, and the values are the means ± SD of three individual experiments.

*p<0.05; **p<0.01; and ***p<0.001.

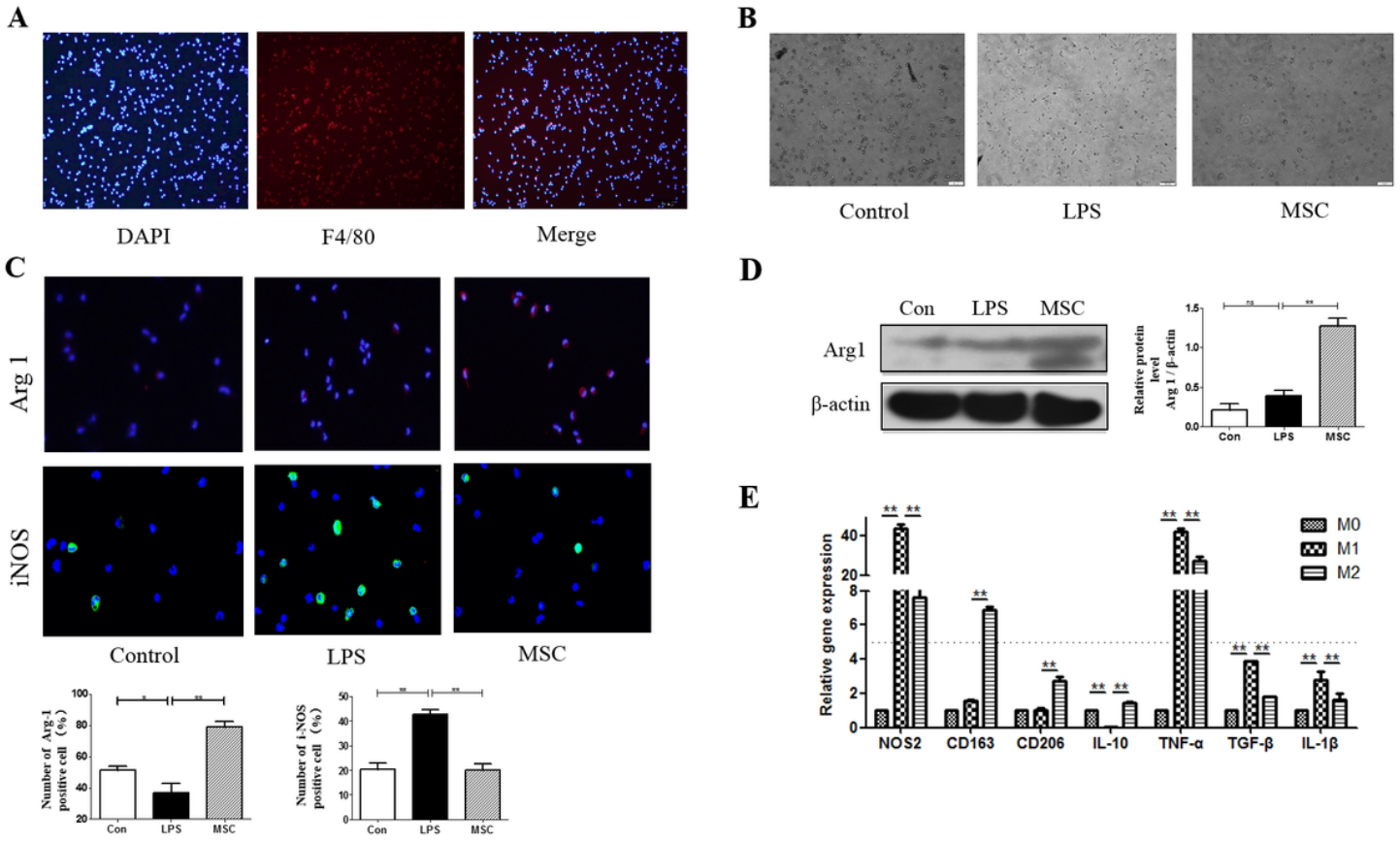

Figure 6

UC-MSCs suppressed M1 macrophage polarization and induced M2 macrophage polarization in vitro.

A Peritoneal macrophages were extracted, and it was verified that more than 95% of the cells were F4/80 positive (red, a marker for macrophages regardless of sub-phenotypes).

B Under a light microscope, LPS administration was observed to induce the extension of many pseudopodia by macrophages. After co-culture with UC-MSCs, fewer acrophage pseudopodia were observed in vitro.

C Immunofluorescence of Arg 1 and iNOS in the control, LPS and MSC groups. Quantification of these markers was evaluated in at least three random fields of each section.

D Immunoblotting analysis of Arg 1 in the three groups. The results are presented relative to those of the control group.

E Quantitative RT-PCR analysis of gene expression in peritoneal macrophages from the three groups.

Data are presented as mean ± SD of three individual experiments. *p<0.05; **p<0.01; and ***p<0.001.

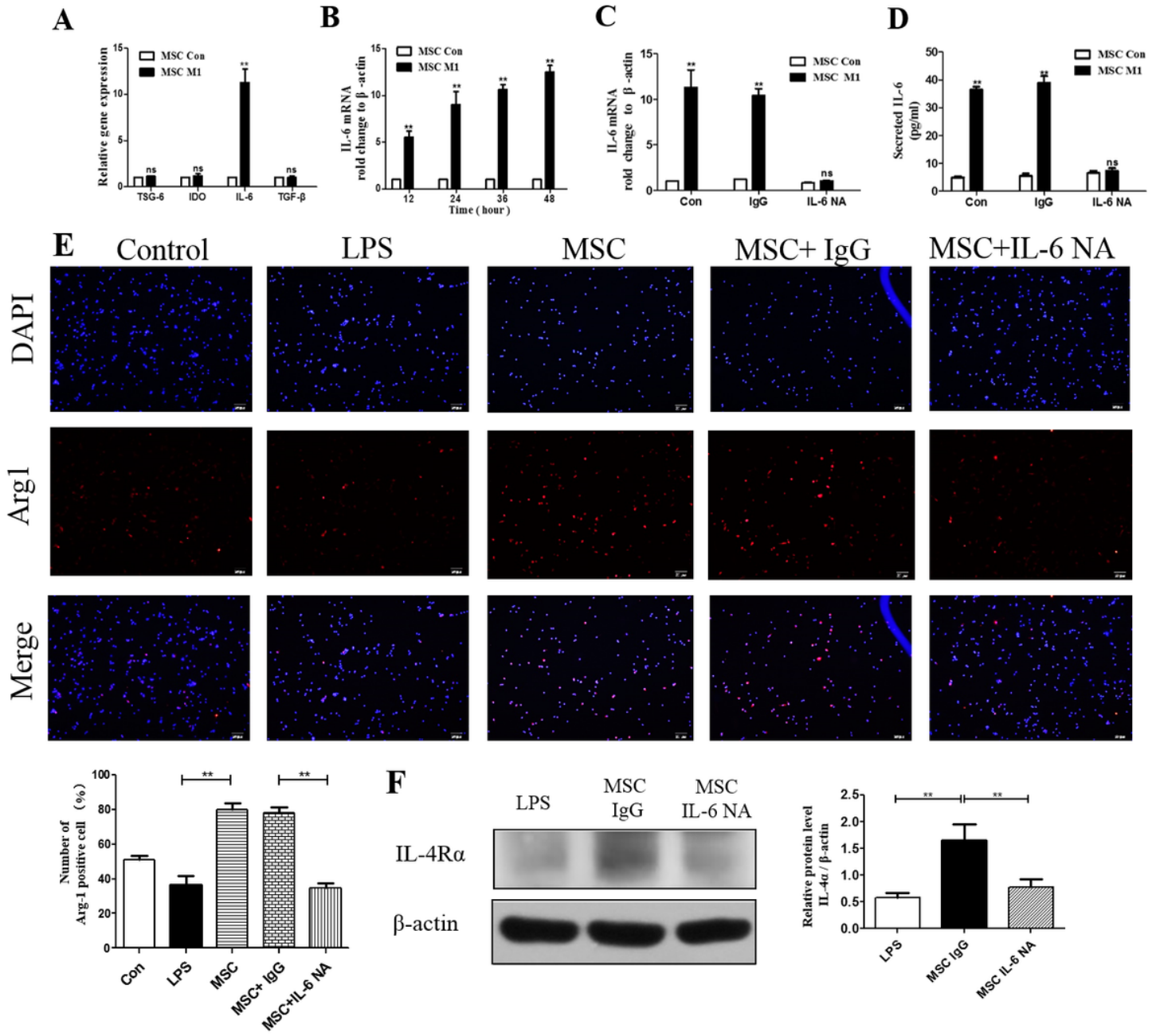

Figure 7

UC-MSCs induced M2 macrophage polarization via IL-6/IL-4R in vitro.

(A) UC-MSCs were cultured with LPS-stimulated macrophages (M1) for 24 h, and the gene expression of the factors secreted by UC-MSCs was detected by quantitative RT-PCR analysis. The control group was UC-MSCs cultured alone.

(B) Quantitative RT-PCR analysis of IL-6 expression in UC-MSCs after co-cultured with LPS-stimulated macrophages (M1) for 12, 24, 36 and 48 h. The control group was UC-MSCs cultured alone.

(C) Quantitative RT-PCR analysis of IL-6 expression in UC-MSCs after co-cultured with LPS-stimulated macrophages (M1) for treatment with IgG or IL-6 neutralizing antibody. The control group was UC-MSCs cultured alone.

(D) Enzyme-linked immunosorbent assays of IL-6 in the medium of UC-MSCs co-cultured with LPS-stimulated macrophages (M1) for treatment with IgG or an IL-6 neutralizing antibody. The control group was UC-MSCs cultured alone.

(E) Immunofluorescence of Arg 1-positive macrophages from control, LPS (peritoneal macrophages stimulated with LPS), MSC (LPS stimulated macrophages co-cultured with UC-MSCs), MSC+IgG (IgG was added to the medium of LPS-stimulated macrophages co-cultured with UC-MSCs), MSC+IL-6 NA (IL-6 neutralizing antibody was added to the medium of LPS-stimulated macrophages co-cultured with UC-MSCs) groups.

(F) Immunoblotting analysis of IL-4Rα in macrophages from LPS, MSC+IgG and MSC+IL-6 NA groups.

Data are presented as mean ± SD and are representative of three independent experiments. *p<0.05; **p<0.01; and ***p<0.001.

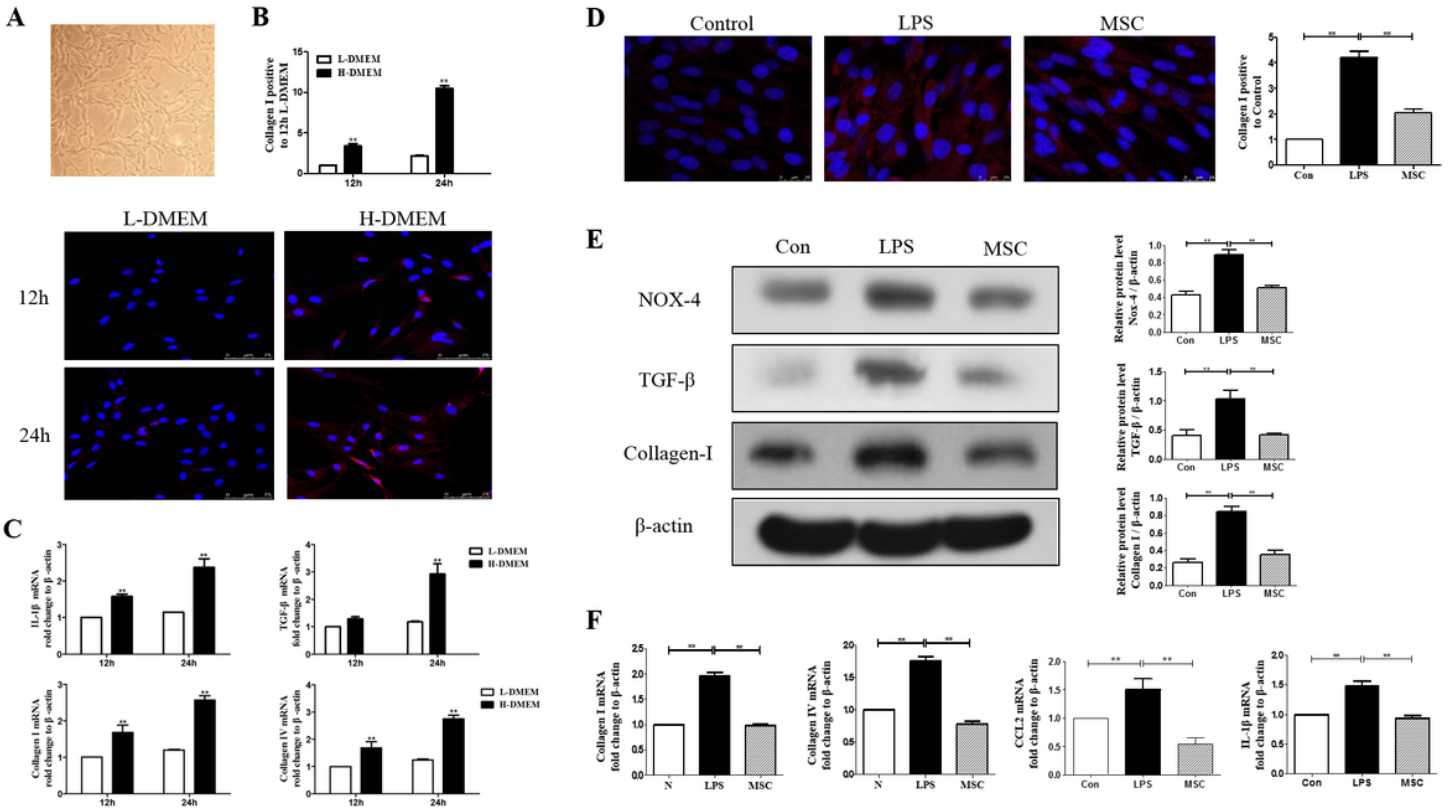

Figure 8

UC-MSCs-induced M2 macrophages protect HBZY-1 from high glucose toxicity.

(A) The morphological characteristics of HBZY-1 cells under a light microscope.

(B) HBZY-1 cultured with L-DMEM or H-DMEM for 12h and 24h were stained with anti-collagen I (red) antibody.

(C) Quantitative RT-PCR analysis of IL-1β, TGF-β, collagen I and collagen IV expression in HBZY-1 cells. The results are presented relative to those of HBZY-1 cultured with L-DMEM for 12 h, set as 1.

(D) Photomicrographs of HBZY-1 stained with anti-collagen I (red) antibody from control (HBZY-1 cultured with H-DMEM for 24ch co-cultured with M0 macrophages), LPS (HBZY-1 cultured with H-DMEM for 24 h co-cultured with LPS-stimulated M1 macrophages), and MSC (HBZY-1 cultured with H-DMEM for 24 h co-cultured with UC-MSCs-induced M2 macrophages) groups.

(E) Immunoblotting analysis of NOX-4, TGF-β and collagen I in HBZY-1 from the control, LPS and MSC groups. Protein levels are presented relative toβ-actin.

(F) Quantitative RT-PCR analysis of collagen I, collagen IV, CCL2 and IL-1βgene expression in HBZY-1 from the control, LPS and MSC groups.

Data are presented as mean ± SD and are representative of three independent experiments. *$p<0.05$; **$p<0.01$; and ***$p<0.001$.

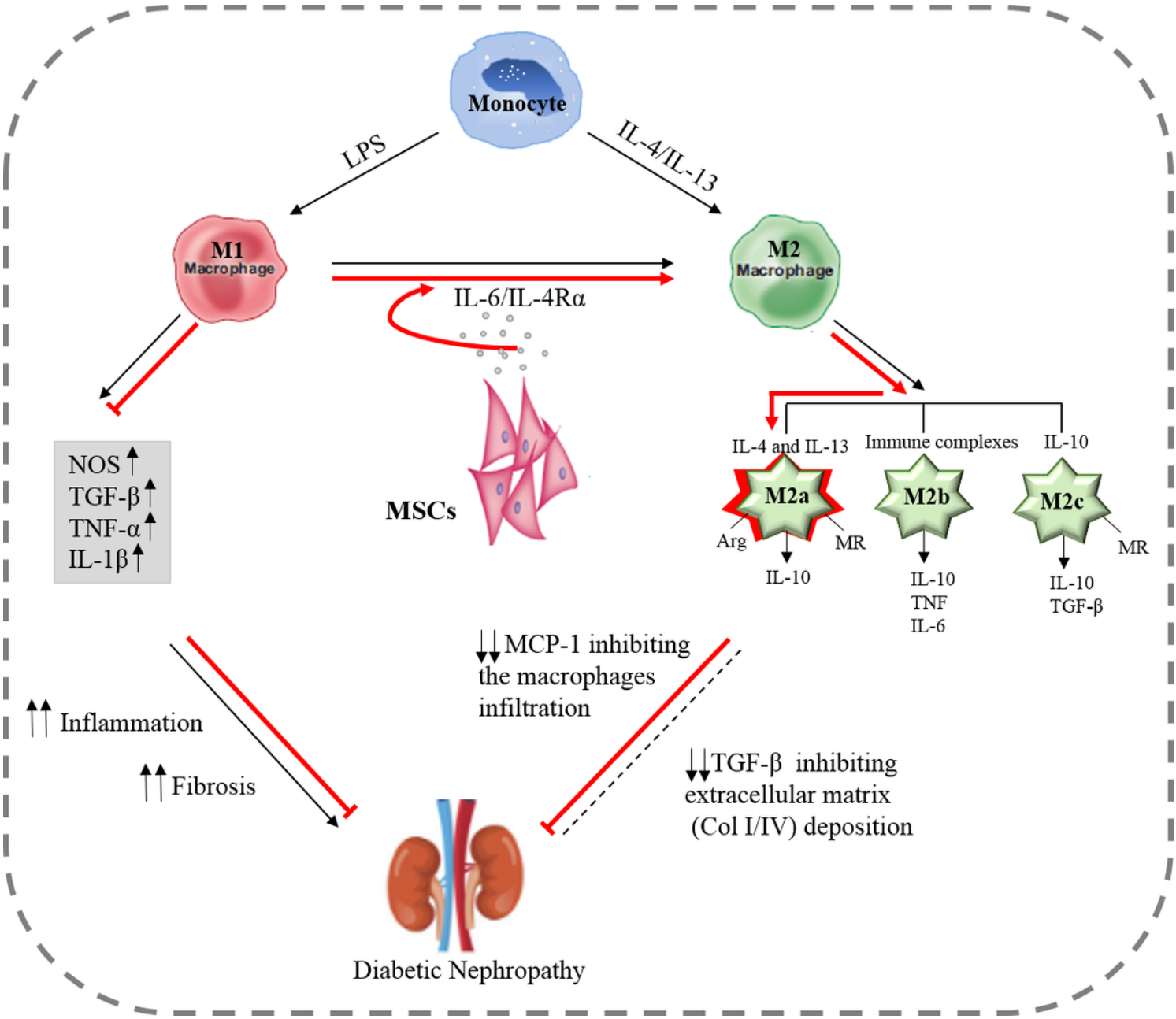

Figure 9

MSCs promotes the polarization of macrophages from M1 to M2a via IL-6/IL-4Rα pathway to ameliorate the inflammation and fibrosis of diabetic nephropathy.

Our study highlighted the regulatory roles macrophages play in the progression of diabetic nephropathy. MSCs administration promotes the polarization of macrophages from M1 to M2a via IL-6/IL-4Rα pathway, thereby ameliorating the inflammation and fibrosis of diabetic nephropathy.

Supplementary Files

This is a list of supplementary files associated with this preprint. Click to download.

- FigurS1.jpg
- SupplementTableS13.docx